

Flexural Behavior of Two-Span Continuous Prestressed Concrete Girders with Highly Eccentric External Tendons

by Thiru Aravinthan, Eakarath Witchukreangkrai, and Hiroshi Mutsuyoshi

It is generally known that the flexural strength of beams prestressed with external tendons is comparatively lower than that of members with internal bonded tendons. One possible method of enhancing the flexural strength of such beams is to place the tendons at high eccentricity. To obtain an insight into the flexural behavior of beams with highly eccentric tendons, an experimental investigation is conducted on single-span and two-span continuous beams. The test variables include external tendon profile, loading pattern on each span, casting method, and confinement reinforcements. It is found that continuous girders with linearly transformed tendon profiles exhibit the same flexural behavior irrespective of tendon layout. The presence of confinement reinforcement enhances the ductility behavior but does not increase the ultimate flexural strength. The degree of moment redistribution is affected by the tendon layout and the loading pattern on each span. The results of the experimental investigation are discussed in this paper.

Keywords: flexure; girders; prestressed concrete.

INTRODUCTION

There has been a tremendous amount of research and development on the use of external tendons in recent years. Applications include new types of composite structures, such as prestressed box girder bridges with corrugated steel webs and truss bridges. Some of the advantages of external prestressing are: 1) the possibility of replacing prestressing tendons; 2) reduction in web thickness due to elimination of tendons within the concrete, resulting in reduced construction cost and lightweight structures; and 3) enhanced construction processes combined with the precast segmental method of construction. Previous research, however, has shown that the flexural strength of externally prestressed beams is comparatively lower than that of similar internal bonded beams.¹⁻⁵ One possible method of enhancing the flexural strength of externally prestressed beams is to make the tendons highly eccentric. When the depth of tendon is greater than the beam height, this could be considered as highly eccentric as opposed to tendons placed within the beam height, which is treated as normal eccentricity. This kind of construction is possible only when external prestressing is used because this allows the tendons to be arranged outside the concrete section.

The Truc de la Fare Bridge⁶ in France was of this type of construction, consisting of a prestressed concrete slab with lateral ribs supported by subtended cables given eccentricity with three steel struts, and has a span of 53 m. A pedestrian bridge of similar design has been constructed in Nagano prefecture, Japan, on an experimental basis, with a span of 40 m.⁷ With these designs, compressive forces are taken by the concrete and tension by the external tendon, thus taking full advantage of both materials. An experimental investigation has been carried out to study the flexural behavior of such

single-span structures by Hamada et al.⁸ Moreover, an experiment was carried out on single-span beams with large eccentricities to study the influence of effective prestressing on the ultimate flexural strength.⁹ It was found that, by increasing tendon eccentricity, strength can be improved or, conversely, the amount of prestressing reduced; the result is more economical structures.

It is believed that extending this concept to continuous girders will lead to improved structural performance and more elegant structures. To obtain an insight into the flexural behavior of such beams, an experimental study was conducted on two-span continuous beams with highly eccentric external tendons. The results of this investigation are presented in this paper, with emphasis on the influence of tendon layout and loading pattern on the ultimate flexural strength and the stress increase in the external tendons. In addition, the effects of confinement reinforcement and casting method on the overall flexural behavior of such beams are also investigated.

RESEARCH SIGNIFICANCE

This paper presents an experimental investigation on the flexural behavior of two-span continuous beams prestressed with highly eccentric external tendons—a subject that has not been explored in the past. The effect of tendon layout, loading pattern, casting method, and confinement reinforcements on the flexural strength and stress in external tendons is discussed. The rate of tendon stress increase is also compared with that of single-span beams. Further, the influence of secondary moment on moment redistribution and the applicability of selected code equations in predicting the redistributed moment for beams used in this study is investigated.

EXPERIMENTAL METHODOLOGY

A series of experiments was carried out using a total of nine beams to investigate the flexural behavior of beams prestressed with highly eccentric external tendons. The test series consisted of six specimens with two-span continuous beams (Types A, B, and C) and three single-span beams (Type D). The two-span continuous beams are 10.4 m long, with two equal spans of 5.0 m, as shown in Fig. 1(a). The specimens are rectangular in cross section throughout their length, having a width of 400 mm and a depth of 150 mm. Seven deviators were fitted: one at the center support and three in each span at a spacing of 1.25 m. The single-span

ACI Structural Journal, V. 102, No. 3, May-June 2005.

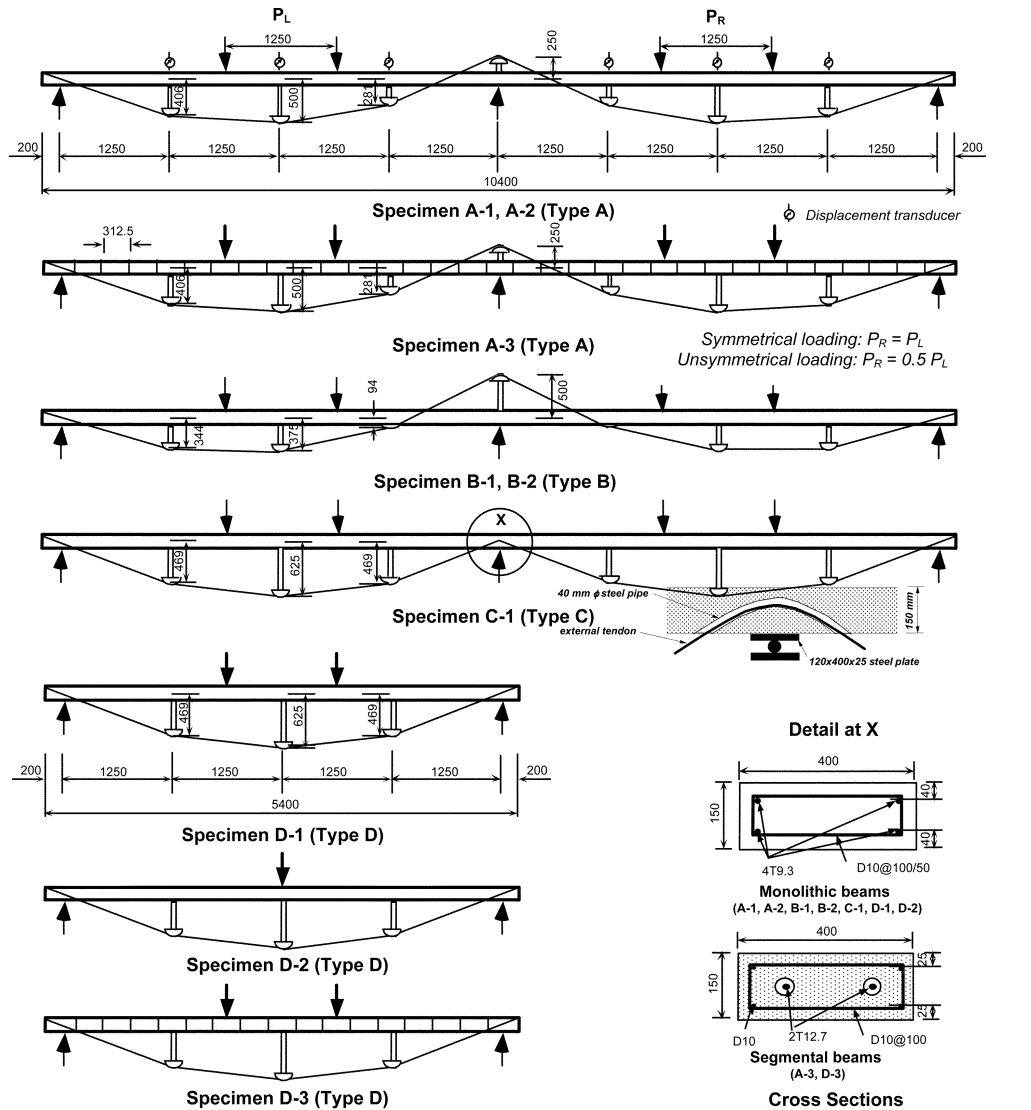
MS No. 03-476 received December 2, 2003, and reviewed under Institute publication policies. Copyright © 2005, American Concrete Institute. All rights reserved, including the making of copies unless permission is obtained from the copyright proprietors. Pertinent discussion including author's closure, if any, will be published in the March-April 2006 *ACI Structural Journal* if the discussion is received by November 1, 2005.

ACI member **Thiru Aravinthan** is a senior lecturer of structural engineering at the University of Southern Queensland, Toowoomba, Queensland, Australia. He received his MEng and DEng from Saitama University, Japan, in 1996 and 1999, respectively. His research interests include strengthening of structures using external post-tensioning, fiber composites, and recycled concrete.

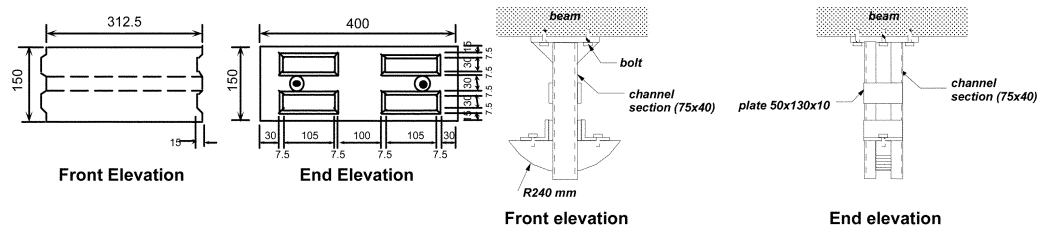
Eakarat Witchukreangkrai is a postdoctoral researcher at Saitama University, where he received his MEng and PhD in 2000 and 2003, respectively. His research interests include strengthening using external prestressing, durability of post-tensioned concrete structures, and partially prestressed concrete structures.

ACI member **Hiroshi Mutsuyoshi** is a professor of civil engineering and Director of the Cooperative Research Center at Saitama University. He is a member of ACI Committee 440, Fiber Reinforced Polymer Reinforcement. His research interests include external prestressing, strengthening of concrete structures, fiber-reinforced polymer reinforcement, and earthquake response of structures.

beams (Type D) had a total length of 5.4 m with a span of 5.0 m, and each had three deviators. The test variables and materials used are given in Table 1. Specimen Types A, B, and C differ in the arrangement of the external tendons. Specimen Type D (single-span beam) has a tendon layout similar to that of specimen Type C (continuous beam). Specimens A-3 and D-3 were made of precast segmental beams, whereas all other beams were of the monolithic type. Specimens B-1, B-2, and C-1 were provided with confinement reinforcement in the concrete compressive zone at critical locations to improve their ductility. Rectangular stirrups made of 10 mm bar were tied at a spacing of 100 mm along the beam. In the loading span and center support region of



(a) Dimension of specimens (in mm)



(b) Shear-key (in mm)

(c) Deviator

Fig. 1—Details of test specimens.

Table 1—Experimental results

No.	Description of specimen	Method of casting	Loading		Tendon eccentricity, mm		Confinement reinforcement (volumetric ratio)	Prestressing tendons*		
			Left span	Right span	Midspan	Center support		Internal tendon	External tendon	
A-1	Two-span continuous beam	Monolithic	100%	100%	500	250	—	1T9.3 × 4 (4 × 50 kN) (56% f_{pu})	1T10.8 × 1 (25 kN) (21% f_{pu})	
A-2			100%	50%						
A-3		Precast segments	100%	100%						
B-1		Monolithic casting	100%	100%	375	500				D10 at 50 (3.2%)
B-2			100%	50%						
C-1			100%	100%	625	0				
D-1	Single-span beam	Two-point			625	—	—	1T9.3 × 4 (4 × 50 kN) (56% f_{pu})		
D-2			One-point							
D-3		Precast segments	Two-point							

*1T denotes single-strand tendon.

Table 2—Mechanical properties of prestressing tendons

Type of tendon	Sectional area, mm ²	Young's modulus, GPa	Yield force,* kN	Ultimate force, kN
SWPR7A-1T9.3 mm	51.61	196.2	76	89
SWPR7B-1T10.8 mm	69.68		102	120
SWPR7B-1T12.4 mm	92.90		136	160

*0.2% proof load, obtained from manufacturer's specifications.

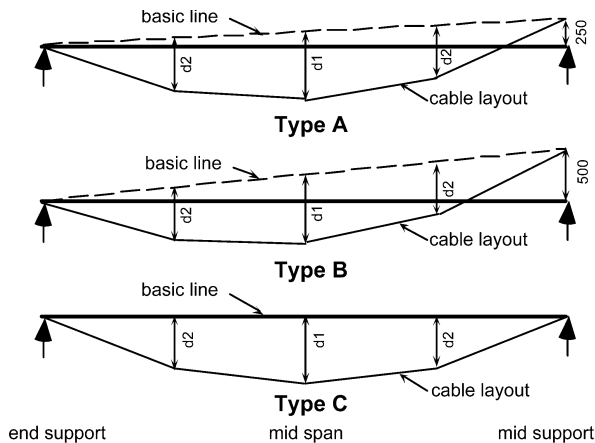


Fig. 2—Linear transformation of tendon layouts.

Specimen Types B and C, stirrups were spaced at 50 mm to behave as confinement reinforcement.

The monolithic beams were provided with combined prestressing consisting of internal bonded tendons and post-tensioned external tendons. The internal tendons consisted of four 9.3 mm SWPR7A standard cables pretensioned and cast monolithically with the specimen. The precast segmental beams incorporated post-tensioned tendons consisting of two 12.4 mm SWPR7A cables. The external tendon layout was designed as described as follows. In the single-span specimens of Type D, the maximum eccentricity of the tendon is 625 mm, giving a span-sag ratio of 8. The tendon position was determined so as to achieve a near-parabolic tendon profile. The same tendon profile was used for the continuous beams of Type C, with no eccentricity at the

center support. The tendon profile in Type A and B specimens was obtained by a linear transformation of the tendon profile of Type C specimen, as shown in Fig. 2. The tendon profile of Type B specimens was close to that of a concordant tendon where there are no secondary moments due to prestressing. The eccentricity at the center support was 500 mm, resulting in a midspan eccentricity of 375 mm. In Type A specimens, the tendon eccentricity at the center support was half that of Type B specimens, at 250 mm, giving a midspan eccentricity of 500 mm. It should be noted that the effect of secondary moments resulting from prestressing is greatest in Type C and least in Type B. The amount of internal prestressing was, in principle, designed to achieve an effective prestress of approximately 200 kN, which was sufficient to support the self-weight of the specimen during handling prior to application of external prestressing. In the case of the monolithically cast beams, however, the design prestress was somewhat higher in consideration of elastic shrinkage during transfer, creep, and other losses.

For ease of casting, specimens were concreted in a vertical orientation; that is, the top and bottom surfaces were cast against the vertical form. Monolithic specimens were cast in the factory and transported to the laboratory for testing. The precast segments with shear keys were cast using the long-line match-casting technique in the factory. They were later assembled in the laboratory using epoxy resin, and the internal prestressing was applied. Details of the shear keys are shown in Fig. 1(b). To simulate the behavior of external tendons placed within the box girder, in Specimen D-3, the internal tendon was left unbonded. The design strength of the concrete was specified as 50 MPa at 14 days. Steel struts were used as deviators, and these were fixed to the beam after it was placed on the supports. Details of the deviator struts are shown in Fig. 1(c). For external prestressing, 10.8 mm-diameter SWPR7B cable was used with a design value of 25 kN. The mechanical properties of the prestressing strands are shown in Table 2 (based on the manufacturer's specifications). A Teflon sheet was inserted between tendons and deviators to reduce friction. In Specimen A-2, grease was also applied between sheet and deviator to further minimize frictional effects. Strain gages were attached to the reinforcement and on the concrete surface at critical locations. To measure strain variations in the tendons, gauges were fixed

Table 3—Summary of experiment results

No.	Cracking load, kN			Ultimate load, kN		Maximum deflection, mm		Ultimate tendon force, kN		Average stress increase, MPa	Concrete strength, MPa	Failure mode	
	Left span	Center support	Right span	Left span	Right span	Left span	Right span	Left end	Right end			Concrete	External tendon
A-1	39.2	36.8	39.2	107.9	108.6	82.7	82.6	117.1	116.6	1306	51.9	Crushing	Yield
A-2	34.2	39.2	—	88.1	47.6	112.7	−24.6	88.3	84.4	870	58.6		No yielding
A-3	38.7	37.7	44.9	97.6	104.0	80.1	80.0	113.3	111.5	1275	60.3		Yield
B-1	39.6	37.0	39.4	108.1	107.6	110.2	110.2	118.3	118.1	1328	57.4		No yielding
B-2	36.8	41.7	—	90.8	49.6	150.2	−31.4	96.1	86.3	1070	59.4		Yield
C-1	41.7	36.8	41.6	109.7	110.9	80.2	80.0	114.4	115.6	1290	54.0		
D-1	37.0 (34.7)*			94.5 (88.6)*		130.3		117.9	118.3	1340	57.2		
D-2	29.2 (36.5)*			82.2 (102.8)*		120.1		117.6	117.9	1371	56.9		
D-3	36.3 (34.0)*			86.3 (80.9)*		100.2		114.4	114.1	1300	70.1		

*Equivalent moments (in kN-m) are given in parentheses.

at various locations along the length. Load cells were placed at the anchorages of the external tendon to measure the tendon force. In the case of continuous beams, load cells were also placed under the beams at each support to obtain the support reactions. Figure 3 shows a continuous beam under testing.

The applied load was measured using load cells installed under the jacks. Displacement transducers were placed at midspan and at the deviators to measure the vertical deformations of the beam. In two-span continuous beams, load was applied at two points at a distance of 1.25 m in each span, as shown in Fig. 1(a). Specimens A-1, A-3, B-1, and C-1 were loaded symmetrically, and Specimens A-2 and B-2 underwent unsymmetrical two-span loading. In beams with unsymmetrical loading, the loading in the right span was set to 50% of that in the left span. This was the minimum loading necessary to prevent failure due to reversal of moments in the lightly loaded span. Loading was stopped when crushing of concrete occurred in the compressive zone at both the midspan and center support. In single-span specimens, two types of loading were carried out. Specimens D-1 and D-3 were loaded at two points, similar to the continuous beams explained previously, while a single-point load at midspan was applied to Specimen D-2.

TEST RESULTS AND DISCUSSION

Load-displacement characteristics

Monolithic beams—The experimental results are summarized in Table 3. The load at the first visible crack in the center support was around 37 kN in symmetrically loaded Specimens A-1, B-1, and C-1. The load was approximately 40 kN when cracking was first observed in the midspan region in the same specimens. In the unsymmetrically loaded specimens, the first crack was observed in the midspan region of the highly loaded left span. This value was approximately 35 kN for Specimens A-2 and B-2. In these specimens, cracking at the center support was observed when the load reached approximately 40 kN. The ultimate load on symmetrically loaded specimens was approximately 108 kN. The figure was approximately 17% lower for the unsymmetrically loaded specimens, at approximately 90 kN. This difference is mainly attributable to the increased tendon stress at the ultimate state, which was considerably small in the unsymmetrically loaded specimens.

In the single-span beam with two loading points (Specimen D-1), the cracking load was approximately 37 kN, while for Specimen D-2 with one loading point, it was approximately



Fig. 3—Testing of continuous beam specimen.

29 kN. It should be noted that though these two loads are different in value, the corresponding moments giving rise to the moment of rupture are approximately the same at approximately 35 kN-m. The ultimate load was approximately 95 and 82 kN corresponding to moments of 89 and 103 kN-m for Specimens D-1 and D-2, respectively. The difference in these moments is approximately 15%. This is attributable to differing tendon eccentricity at the critical section, which was 547 and 625 mm in Specimens D-1 and D-2, respectively; this ratio is similar to the ratio of the ultimate moments. The failure mode of all specimens was crushing of the concrete at the critical section. Crushing was observed in the top fibers of the midspan directly under the loading point in all specimens. In addition, crushing was also observed in Specimen C-1 near the center support in the bottom fibers at the location where the cross-sectional area was reduced to make provision for the pipe to carry the external tendon.

Comparing the applied moment with midspan displacement in single-span specimens in Fig. 4(a), it can be seen that the moment capacity of Specimen D-2 was higher than that of Specimen D-1. This is attributable to the difference in tendon eccentricity at the critical section. The load-displacement characteristics of continuous-span specimens with symmetrical loading are compared in Fig. 4(b). It can be seen that the flexural behavior of Specimens A-1 and B-1 was almost identical up to crushing of the concrete. Specimen C-1 also exhibited almost the same behavior, but with a slightly higher stiffness. This difference can be attributed to

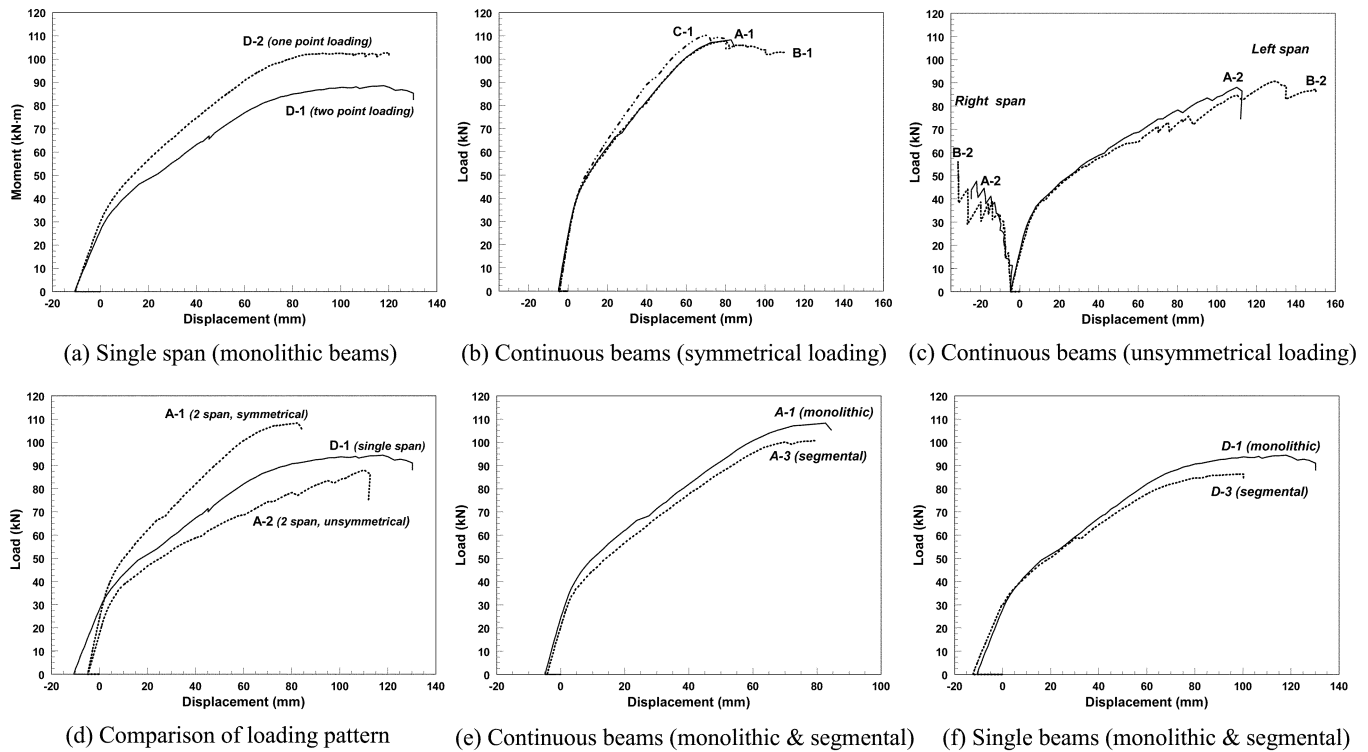


Fig. 4—Load-displacement characteristics.

the slight adjustment made in tendon position in the case of C-1 at the center support; this was necessary to avoid sharp curvature of the cable. In Specimen B-1, which had confinement reinforcement, following spalling of concrete in the midspan region, it remained able to sustain loading with further deformation. In the other confined specimen, C-1, however, loading was stopped due to premature crushing of concrete near the center support. This is believed to have been caused by the provision of a relatively large steel pipe (40 mm diameter) that required cutting of some of the confinement reinforcement; as a result, confinement may not have been effective. Likewise, the unsymmetrically loaded Specimens A-2 and B-2 exhibited similar flexural behavior, as shown in Fig. 4(c). The confined Specimen B-2 underwent greater displacement than unconfined Specimen A-2.

In continuous beams with unsymmetrical loading, the heavily loaded left span showed a downward deflection, while the lightly loaded right span had an upward deformation. From the values of displacement summarized in Table 3, it can be seen that the ultimate deflections of confined Specimens B-1 and B-2 were approximately 33% greater than those of unconfined Specimens A-1 and A-2. A comparison of the behavior of continuous beams and single-span beam, as shown in Fig. 4(d), reveals that the symmetrical loading condition gives the greatest capacity, and that unsymmetrical loading leads to the least load-carrying capacity. The higher load supportable by symmetrically loaded continuous beams is attributable to the structural improvement arising from continuity. The reduced load capacity in unsymmetrical loading, however, results from the smaller stress increase in the external tendon at the ultimate stage.

Segmental beams—The cracking load in continuous-span segmental Specimen A-3 was approximately 37 and 42 kN at the center support and midspan, respectively. In single-span Specimen D-3, this load was 36 kN in the midspan region. This load is nearly the same as for similar mono-

lithically cast beams. It should be noted, however, that crack propagation in the segmental beams was localized in the vicinity of the joints, whereas it was distributed in the monolithic beams. Considering the ultimate capacity, the maximum load of the continuous-span segmental Beam A-3 was 101 kN—approximately 7% less than that of the monolithic beams. The reason for this lower value may be due to the smaller area of the internal bonded tendons, as well as the slight reduction in initial prestress in the case of precast segments. In single-span beam D-3, this load was 86 kN—approximately 9% smaller than in the case of Specimen D-1. This reduction is attributable to the reduced internal tendon area, as well as the use of unbonded tendons. The load-displacement characteristics of segmental and monolithic beams are compared in Fig. 4(e) and (f). It can be seen that the behavior of continuous Specimens A-1 and A-3 was almost the same. For single-span beams, the ultimate deflection was approximately 30% smaller in the segmental beam (D-3) compared to the monolithic beam (D-1). This is mainly attributable to the use of internal unbonded tendons in Specimen D-3 as opposed to an internal bonded tendon in D-1. If Specimen D-3 was provided with an internal bonded tendon, it would have shown a similar flexural behavior to that of D-1.

From the aforementioned observations, it is concluded that in continuous beams with linearly transformed tendon profiles, the flexural behavior is unaffected by tendon layout in both linear elastic and ultimate limit state. This gives considerable flexibility in the design of tendon layouts for beams with highly eccentric external tendons, allowing the tendon eccentricity to be extended below the beam at midspan or above the beam at the support, depending on the clearance available at a particular site. Further, the method by which such beams are cast, either monolithic or precast, has little influence on overall flexural behavior provided that other parameters are kept the same.

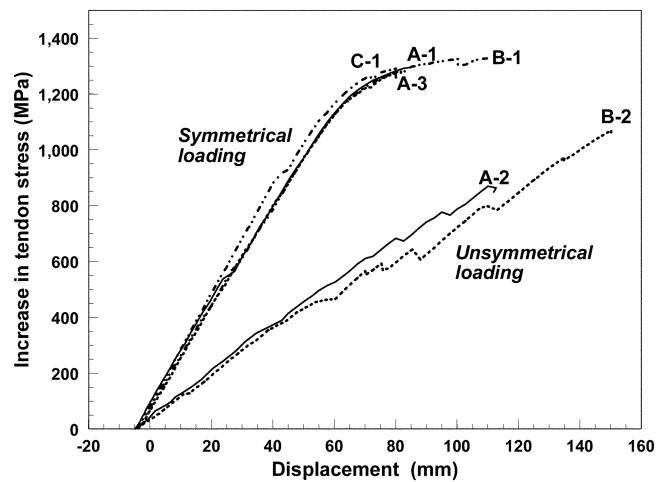
Increase in external tendon stress

The increase in external tendon stress with midspan displacement is shown in Fig. 5(a) for continuous beams. There was no yielding of external tendons in specimens with unsymmetrical loading (A-2 and B-2). In specimens with symmetrical loading (A-1, A-3, B-1, and C-1), however, yielding was observed in the external tendons. Yielding of the tendon was deduced through strain gauge and load cell readings. The tendon was considered to be yielded when the force in the tendon exceeded 0.2% proof load. The observed ultimate tendon forces are summarized in Table 3. In Specimen B-2, it was noted that there was a difference of approximately 10% between the tendon force measured at the left and right ends. This is believed to arise because of frictional effects at the deviators due to the large angle of deviation, especially at the center support. This difference falls to 4% in Specimen A-2, where grease was applied between the deviators and teflon sheet. In other continuous-beam and single-span beam specimens, this difference was found to be insignificant at less than 1%. Specimens with symmetrical loading had a larger ultimate tendon stress than those with unsymmetrical loading. This can be attributed to the fact that under symmetrical loading, both spans had a considerable deflection, thus substantially increasing the elongation of the tendon. In unsymmetrical loading, however, while the left span underwent a downward deflection, the right span experienced upward deformation, thus having a negative impact on the increase in tendon force.

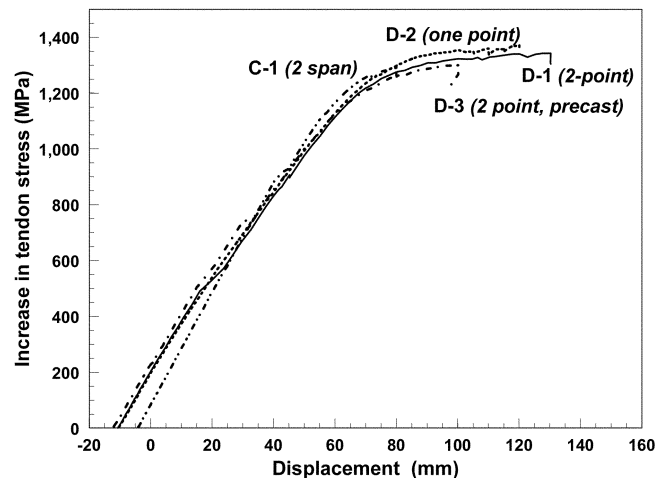
It can be seen from Fig. 5(a) that the stress increases in a nearly linear manner up to yielding, following almost the same path as specimens with symmetrical loading. Similar behavior was observed in unsymmetrically loaded specimens. As such, it can be inferred that there is a direct relationship between tendon force increase and midspan displacement. The rate of increase in stress under symmetrical loading was approximately 17.5 MPa/mm. The corresponding value for unsymmetrical loading was 7.5 MPa/mm—less than half of the symmetrical loading value. It can be concluded that the tendon stress increase is directly proportional to the midspan deflection. Further, the rate of change of this stress is influenced by the loading arrangement in each span. Considering the stress increase in single-span beams as shown in Fig. 5(b), it can be seen that Specimens D-1, D-2, and D-3 behave similarly. Comparing this behavior with symmetrically loaded continuous Beam C-1, it is seen that the behavior is almost identical. This indicates that the rate of increase in tendon stress of single-span beams and continuous beams is nearly the same, and supports the approach used in the design equation for continuous beams as proposed in some previous studies (Aravinthan et al.;¹⁰ Naaman and Alkhairi¹¹).

Secondary moments at ultimate limit state in continuous beams

In continuous beams with nonconcordant tendon profiles, prestressing generally induces reactions at the supports. As a result, the supports exert reactions on the beam, causing the secondary moments. The observed change in support reactions with the applied prestress is given in Fig. 6, neglecting the self-weight and equipment loads initially present on the beam. It can be seen that the reaction at the center support falls gradually, while at the end supports, the reaction increases. This effect was most significant in Type C specimens and least visible in Type B specimens. This is



(a) Continuous beams



(b) Single-span beams

Fig. 5—Stress increase in external tendons with midspan deflection.

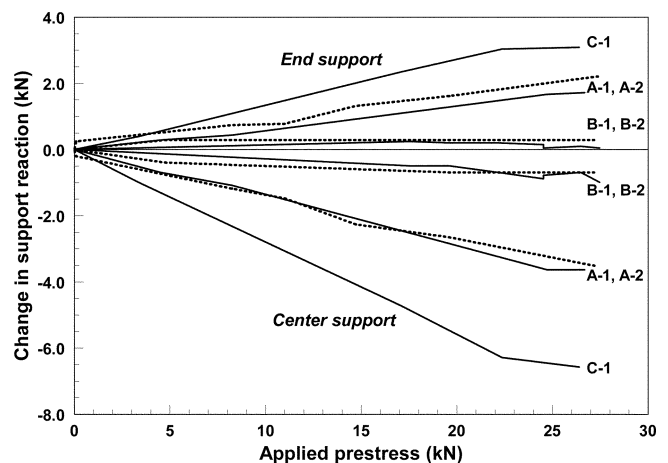


Fig. 6—Change in support reaction with introduced prestress.

attributable to the layout of the tendons in these specimens; in Type B, they were nearly concordant.

The behavior of secondary moments in the post-elastic region of continuous prestressed concrete beams has been a subject of considerable controversy for many years, and no

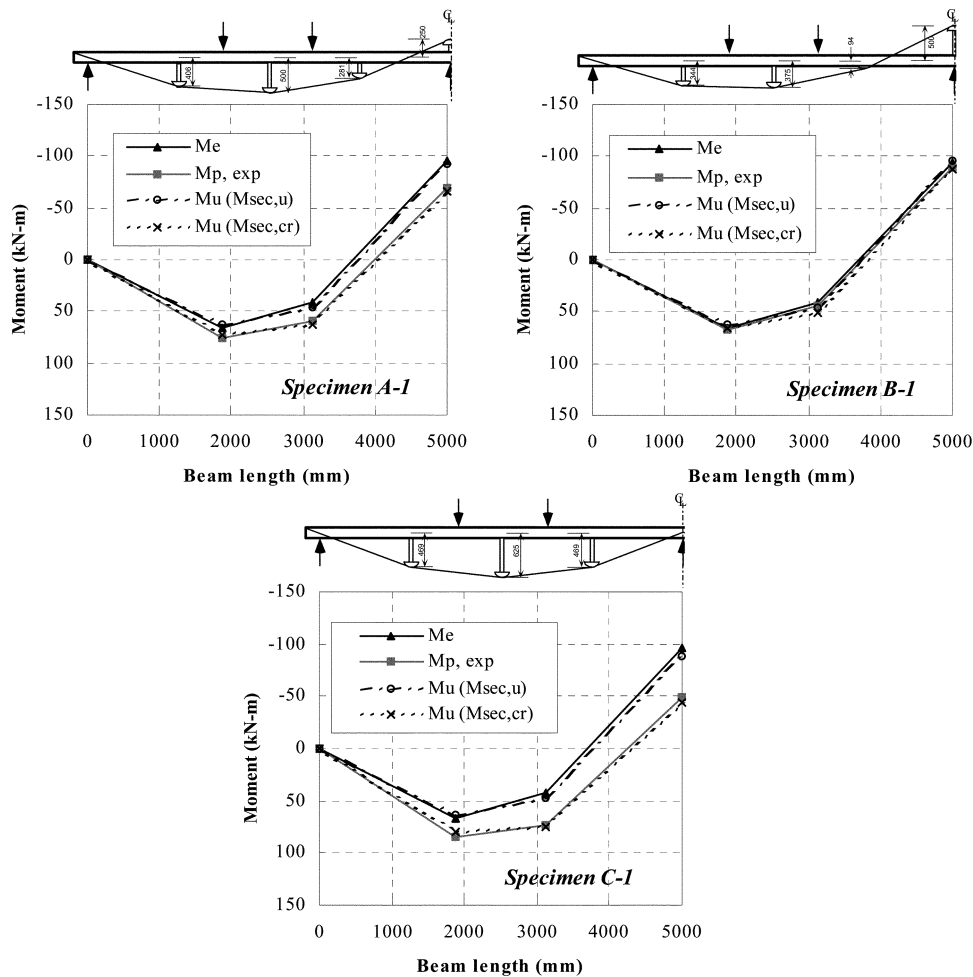


Fig. 7—Secondary moments at ultimate limit state (symmetrical loading).

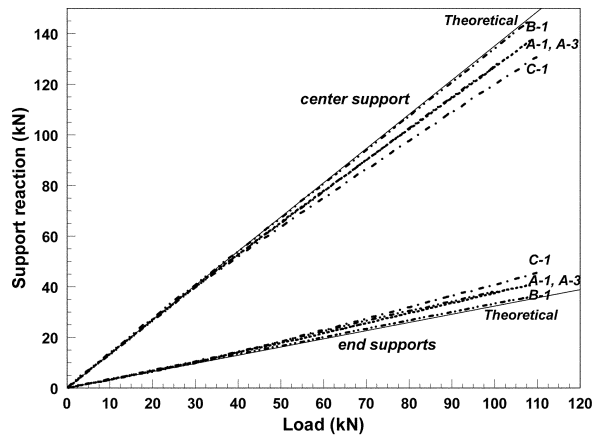
general conclusions have yet been reached. This includes lack of agreement as to whether the secondary moment should be considered in determining the ultimate moment capacity M_u of the critical section in a continuous prestressed concrete beam. In ACI 318-71,¹² it is prescribed that the effect of the secondary moment should be neglected when calculating the design moments. This is explained by stating that the secondary moments produced by the prestress in a nonconcordant tendon would disappear after a plastic hinge forms at the center support, and the structure then becomes statically determinate. Inclusion of the secondary moment, however, came about later in ACI 318-95.¹³ There, it is stated that the moment used in computing the required strength shall be the sum of the moments due to factored loads and the secondary moment with a load factor of 1.0. Studies with internal bonded tendons by previous researchers (Wyche, Uren, and Reynolds¹⁴; Mattock¹⁵) have also shown that the prestress secondary moments can be considered present at the ultimate limit state, and that they are often beneficial. Moreover, it was also pointed out that the calculated design moment could be nonconservative when the secondary moments are neglected.

To check the existence of a secondary moment M_{sec} at the ultimate state, the moment capacities at critical sections (loading points and center support) of continuous-span specimens with symmetrical loading (A-1, B-1, and C-1) were calculated assuming two differing magnitudes of secondary moment: 1) at ultimate load $M_{sec,u}$; and 2) at

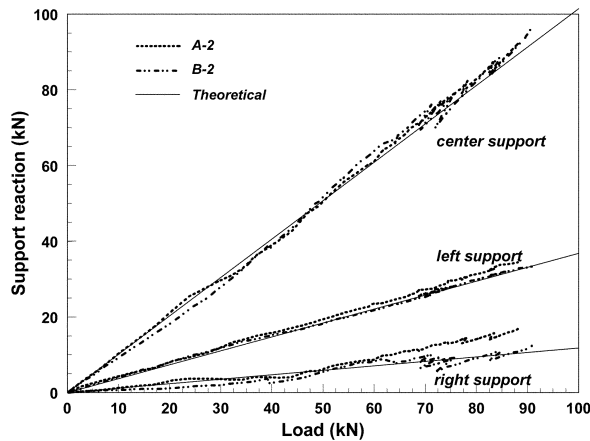
cracking load $M_{sec,cr}$. These secondary moments were determined based on the elastic theory using forces in external tendon corresponding to each load level (ultimate load and cracking load). The resulting calculated moments are compared with those from elastic analysis M_e and with actual moments observed from the experiment $M_{p,exp}$ as shown in Fig. 7. It can be seen that, except for Beam B-1, which had the lowest secondary moment, the ultimate moments computed based on the secondary moments at ultimate load $M_{sec,u}$ diverge greatly from the experimental observations at critical sections. In contrast, the assumption of secondary moment at cracking load $M_{sec,cr}$ shows very good agreement with the experimental results. The reason may be that after the occurrence of cracking at the center support, the secondary moment does not change much due to the fact that the restrained rotation at the center support does not exist anymore. From these results, it can be concluded that the secondary moments determined based on the external tendon force at cracking load shall be considered in the calculation of moment capacity of continuous beams with highly eccentric external tendons.

Moment redistribution in continuous beams

In continuous-span beams, a redistribution of moments can be expected after the critical section reaches the yield moment. If the beam behaves elastically, the variations in support reactions with load will exhibit linear behavior. When this is not so, moment redistribution may take place



(a) Symmetrical loading

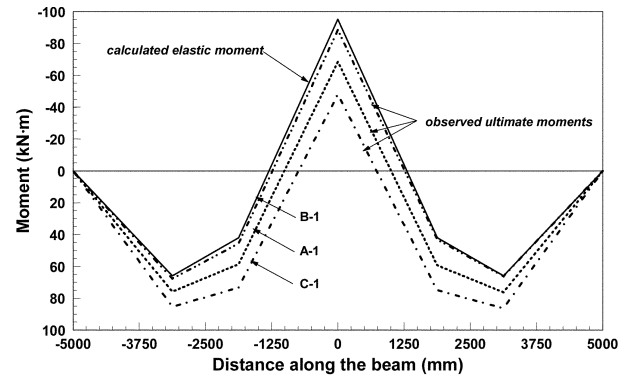


(b) Unsymmetrical loading

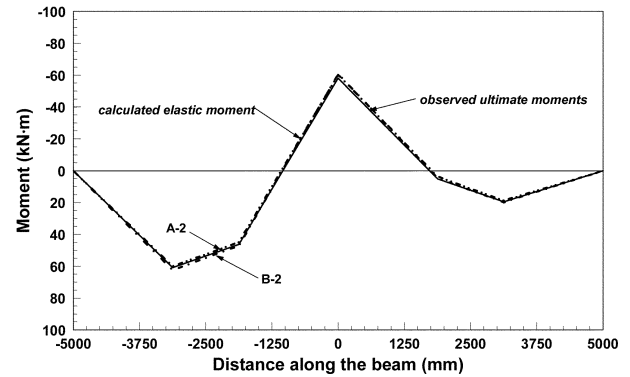
Fig. 8—Change in support reaction with applied load.

from the yielded section to the unyielded sections. To verify these phenomena, the support reactions were measured. Changes in support reaction with applied load are illustrated in Fig. 8(a) and (b). It can be seen that behavior is nearly bilinear. The initial linear range reflects the elastic behavior of the structure, whereas the second part represents the nonlinear behavior. It was observed that the first plastic hinge formed in the center support region in the case of symmetrically loaded specimens because the ratio of moment capacity to applied load was lower at the center support compared with the midspan section. In unsymmetrical loading, the first plastic hinge was observed to the left of the midspan region. As such, the moments were redistributed towards the center support in these beams. From the support reactions, the ultimate plastic moments M_p were calculated at critical sections. The corresponding elastic moments M_e were computed assuming linear behavior. The moment redistribution ratio was calculated from this, and the results are summarized in Table 4. The bending moment profile along the beam was computed from the observed support reactions, as shown in Fig. 9(a) and (b).

It can be seen from Table 4 that, in symmetrical loading, the observed moment at the midspan was generally higher than the elastic moments, indicating a negative redistribution. On the other hand, the support moments were lower than the calculated elastic moments, leading to a positive redistribution of moments. In unsymmetrical loading, the opposite behavior



(a) Symmetrical loading



(b) Unsymmetrical loading

Fig. 9—Moment redistribution in continuous beams.

is observed, though the effect was considerably smaller. Specimens of Type C showed the largest redistribution, while this effect was least in Type B specimens. This is attributed to the difference in tendon layout and to the amount of secondary moment in these specimens. From the aforementioned observations, it can be inferred that moment redistribution in continuous beams is influenced by tendon layout as well as by the loading arrangement in each span.

Evaluation of existing design codes for moment redistribution

To account for the effect of moment redistribution, many code provisions adopt the concept that the required moment at any section is to be calculated by elastic theory and may be increased or reduced by an allowable redistributed moment M_{red} . The current design code recommendations for the percentage of this moment redistribution α are as follows

American Code (ACI 318-95)¹³

$$\alpha \leq 20 \left[1 - \frac{\omega_p + \frac{d}{d_p}(\omega - \omega')}{0.36\beta_1} \right] \quad (1)$$

Canadian Code (A23.3-M84)¹⁶

$$\alpha \leq 30 - 50 \frac{c}{d} \leq 20\% \quad (2)$$

Table 4—Summary of ultimate moments and percentage of moment redistribution

No.	Loading type	Observed plastic moments M_p , kN-m			Calculated elastic moments M_e , kN-m			Moment redistribution $[1 - M_p/M_e]$, %		
		Left span	Center support	Right span	Left span	Center support	Right span	Left span	Center support	Right span
A-1	Symmetrical	75.8	-68.5	76.2	65.8	-95.2	65.8	-15.2	28.0	-15.7
A-2	Unsymmetrical	60.0	-60.2	—	60.8	-58.1	—	1.3	-3.7	—
A-3	Symmetrical	69.9	-63.7	69.8	58.6	-93.8	58.6	-19.3	32.0	-19.1
B-1	Symmetrical	67.7	-88.5	66.2	65.4	-94.6	65.4	-3.5	6.4	-1.2
B-2	Unsymmetrical	62.4	-60.8	—	62.7	-59.9	—	0.6	-1.6	—
C-1	Symmetrical	85.3	-48.1	86.3	67.0	-96.9	67.0	-27.3	50.4	-28.7

Table 5—Comparison of moment redistribution predicted by various design codes with experimental results (symmetrical loading)

No.	Moment and center support, kN-m				Percentage moment redistribution α , %			
	M_p	M_e	M_{red}	M_{sec}	Exp.	ACI	BS	Canada
A-1	68.5	95.2	26.7	37.8	28.0	16.5	20.0	20.0
B-1	88.5	94.6	6.1	11.1	6.4	18.0	20.0	20.0
C-1	48.1	96.9	48.8	63.5	50.4	6.4	20.0	15.6

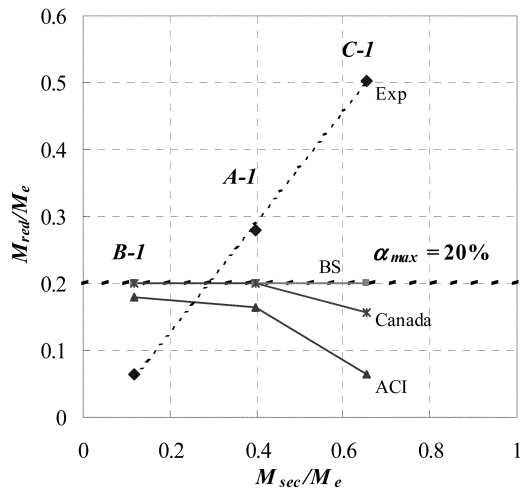


Fig. 10—Moment redistribution versus secondary moment (symmetrical loading).

British Code (BS8110)¹⁷

$$\alpha \leq 50 - 100 \frac{c}{d} \leq 20\% \quad (3)$$

where α is the allowable percentage redistribution of the support moment calculated by elastic analysis; c/d is the neutral axis depth ratio of the section at the ultimate limit state; ω_p , ω , and ω' are reinforcement indexes for prestressing reinforcement, tensile nonprestressing reinforcement, and compressive nonprestressing reinforcement, respectively; d and d_p are the effective depths of the prestressed and nonprestressed reinforcement, respectively; and β_1 is the equivalent rectangular stress block coefficient.

A comparison of the percentage moment redistribution α , predicted by the various design codes with values observed in the tests on two-span continuous beams with symmetrical loading, is summarized in Table 5 and Fig. 10. It can be seen that Specimen C-1, with the highest secondary moment of all beams, exhibited the largest redistributed moment. Further, the amount of moment redistribution decreases with secondary moment in an almost linear manner. This clearly indicates

that the secondary moment and moment redistribution are related in the same way to relative rotations of the section at the center support. Thus, a higher secondary moment causes greater rotational capacity of the section at the center support and, consequently, greater moment redistribution at the ultimate state. It is important to note that all codes give unconservative results for Specimen B-1, where the amount of secondary moment is the least. This may be attributed to the large eccentricity of the external tendon at the center support in such a beam, thus leading to a low c/d and, consequently, to a high degree of moment redistribution α . In contrast, the moment redistributions predicted by all design codes for the other beams are rather conservative. This is particularly true for Specimen C-1, where the relationship between moment redistribution and secondary moment as calculated by all design codes is inconsistent with the experimental results, where beams with high secondary moments exhibited large moment redistributions. This may be attributed to the fact that the parameters included in the various design codes are related only to the sectional properties of the critical section at the center support (ω_p , ω , ω' , and c/d), so they fail to take into account the influence of the secondary moment, which is structure-dependent. This is in agreement with an earlier study by Kodur and Campbell.¹⁸ As such, it is believed that the effect of secondary moment should be considered in the calculation of moment redistribution, particularly in beams with large eccentric external tendons where the secondary moment is rather high as compared with beams with typical external tendons.

DESIGN CONSIDERATIONS FOR BEAMS WITH HIGHLY ECCENTRIC EXTERNAL TENDONS

In typical girders with external prestressing, the tendon is generally placed within the beam's depth. The design of such beams can be carried out successfully with the existing design methodology. In cases where the tendons have relatively high eccentricity, however, as in the specimens studied in this investigation, there is considerable increase in tendon stress even before cracking takes place. Just prior to observation of the initial crack, the increase in tendon stress was found to be approximately 200 MPa in symmetrically loaded continuous beams, while in unsymmetrically loaded beams, it was approximately 130 MPa. This is much higher than in typical structures with external prestressing. Further, while the external tendon does not yield at the ultimate limit state in a typical structure, in the highly eccentric case, the tendon generally yields. The only exceptions in the tests were the unsymmetrically loaded continuous beams, where yielding was not observed. Given these results, it is necessary to take this behavior into consideration when designing structures with large eccentricities.

Another factor to be considered is the frictional effects at the deviators. In typical structures, the angle of deviation is small, and the frictional effects can be safely neglected in normal design. In highly eccentric structures, however, there can be considerable frictional effect as a result of the large angle of deviation in the tendons. This is especially true in continuous beams with unsymmetrical loading. It is therefore necessary to consider these effects in the design of such structures. Further study is recommended to evaluate the suitability of existing design methodologies for the application of prestressed concrete beams with highly eccentric external tendons.

SUMMARY AND CONCLUSIONS

An experimental investigation was conducted on two-span continuous prestressed concrete beams with highly eccentric external tendons. The major variables were the tendon layout, based on linear transformations, and the loading pattern on each span. For comparison purposes, tests were also carried out on single-span beams to study the influence of the type of loading (two-point and one-point loading) on the ultimate flexural capacity and the stress increase in external tendons. The following conclusions are drawn from this study:

1. The flexural behavior of beams is not affected by the linear transformation of tendon layout in both elastic and post-elastic loading ranges. The presence of confinement reinforcement enhances the ductility behavior but does not increase the ultimate strength of such beams;

2. Yielding of external tendons was observed in specimens with full loading on both spans. Tendon stress increases proportionally with midspan deformation until tendons yield. The rate of increase is influenced by the type of loading arrangement; that is, the ultimate flexural strength of unsymmetrically loaded beams is approximately 20% less than that of symmetrically loaded beams;

3. Frictional effects at the deviators had some effect in the case of unsymmetrically loaded beams due to the large deviation angle of the external tendons. Further, the stress increase in single-span beams was nearly the same as that of symmetrically loaded continuous beams, which supports previous findings by the authors;

4. Considering moment redistribution, midspan sections showed a negative redistribution, while the support section exhibited a positive value in symmetrical loading. The amount of moment redistribution is affected by the tendon layout and loading pattern on each span. In symmetrically loaded beams, the moment redistribution decreases with the secondary moment in an almost linear manner. In the case of unsymmetrical loading, in contrast, moment redistribution is found to be insignificant; and

5. Regarding the design methodology for such structures, further research is needed on the prediction of tendon stress under service loading and at the ultimate stage. Additional research is also recommended on the shear behavior of such beams with different types of strut arrangements.

ACKNOWLEDGMENTS

This research was part of a collaborative research effort funded by DPS Bridge Works Co. Ltd., Tokyo and Mitsui Construction Co. Ltd., Tokyo. The financial and technical support provided by these two organizations for the experimental investigation is gratefully acknowledged.

NOTATION

c = neutral axis depth at ultimate limit state
 d = effective depth of reinforcing steels

d_p = effective depth of prestressing steels
 M_e = moment calculated by elastic analysis
 M_p = moment calculated by plastic analysis
 M_{red} = moment redistribution
 M_{sec} = secondary moment due to prestress
 $M_{sec,cr}$ = secondary moment due to prestress at cracking load
 $M_{sec,u}$ = secondary moment due to prestress at ultimate load
 α = allowable percentage of redistribution of support moment
 β_1 = equivalent rectangular stress block coefficient
 ω = reinforcement index for tension nonprestressed reinforcements
 ω' = reinforcement index for compression nonprestressed reinforcements
 ω_p = reinforcement index for prestressing steels

REFERENCES

- Matupayont, S.; Mutsuyoshi, H.; and Machida, A., "Loss of Tendon's Eccentricity in Externally Prestressed Concrete Beam," *Transactions of JCI*, V. 16, 1994, pp. 403-410.
- Tsuchida, K.; Mutsuyoshi, H.; Matupayont, S.; and Taniguchi, H., "Flexural Behavior of External PC Beams," *Transactions of JCI*, V. 16, No. 2, June 1994, pp. 1009-1014.
- Harajli, M. H., "Strengthening of Concrete Beams by External Prestressing," *PCI Journal*, V. 38, No. 6, 1993, pp. 76-88.
- Harajli, M.; Khairallah, N.; and Nassif, H., "Externally Prestressed Members: Evaluation of Second-Order Effects," *Journal of Structural Engineering*, ASCE, V. 125, No. 10, Oct. 1999, pp. 1151-1161.
- Tan, K.-H., and Ng, C.-K., "Effect of Deviators and Tendon Configuration on Behavior of Externally Prestressed Beams," *ACI Structural Journal*, V. 94, No. 1, Jan.-Feb. 1997, pp. 13-22.
- Virlogeux, M. P., "The Truc de la Fare Bridge," *Proceedings of FIP*, XIIth Congress, Washington, D.C., 1994, pp. F133-F138.
- Ohnuma, K.; Hori, T.; Ukegawa, R.; and Ohshida, H., "Design and Construction of Self-Anchored Suspended Bridge," *Proceedings of the 8th Symposium on Developments in Prestressed Concrete*, Japan Prestressed Concrete Engineering Association, Oct. 1998, pp. 619-624.
- Hamada, Y.; Takemoto, S.; Watanabe, M.; and Shinozaki, H., "Study on Flexural Behavior of PC Cable Truss Bridge," *Proceedings of 7th Symposium on Developments in Prestressed Concrete*, Akita, Oct. 1997, pp. 437-442.
- Aravinthan, T.; Mutsuyoshi, H.; Niitsu, T.; and Chen, A., "Flexural Behavior of Externally Prestressed Beams with Large Eccentricities," *Transactions of JCI*, V. 20, No. 3, July 1998, pp. 673-678.
- Aravinthan, T.; Mutsuyoshi, H.; Atsushi, F.; and Hishiki, Y., "Prediction of the Ultimate Flexural Strength of Externally Prestressed PC Beams," *Proceedings of the 7th Symposium on Development in Prestressed Concrete*, Japan Prestressed Concrete Engineering Association, 1997, Akita, Oct. 1997, pp. 287-292.
- Naaman, A., and Alkhairi, M., "Stress at Ultimate in Unbonded Post-Tensioning Tendons: Part 2—Proposed Methodology," *ACI Structural Journal*, V. 88, No. 6, Nov.-Dec. 1991, pp. 683-692.
- ACI Committee 318, "Code Requirements for Reinforced Concrete (ACI 318-71)," American Concrete Institute, Farmington Hills, Mich., 1971, 78 pp.
- ACI Committee 318, "Building Code Requirements for Structural Concrete (ACI 318-95) and Commentary (318R-95)," American Concrete Institute, Farmington Hills, Mich., 1995, 369 pp.
- Wyche, P. J.; Uren, J. G.; and Reynolds, G. C., "Interaction between Prestress Secondary Moments, Moment Redistribution, and Ductility—A Treatise on the Australian Concrete Codes," *ACI Structural Journal*, V. 89, No. 1, Jan.-Feb. 1992, pp. 57-70.
- Mattock, A. H., "Secondary Moments and Moment Redistribution in ACI 318-77 Code," *Proceedings of the International Symposium on Nonlinearity and Continuity in Prestressed Concrete*, Preliminary Publication 3, University of Waterloo, Canada, 1983, pp. 27-48.
- Canadian Standards Association, "Code for the Design of Concrete Structures for Buildings (CAN3-A23.3-M84)," Rexdale, Ontario, Canada, 1984, 281 pp.
- British Standards Institution, "The Structural Use of Concrete: Part 1, Code of Practice for Design and Construction," BS 8110: Part 1, London, 1985, 99 pp.
- Kodur, V. K. R., and Campbell, T. I., "Evaluation of Moment Redistribution in a Two-Span Continuous Prestressed Concrete Beam," *ACI Structural Journal*, V. 93, No. 6, Nov.-Dec. 1996, pp. 721-728.
- ACI Committee 318, "Building Code Requirements for Reinforced Concrete (ACI 318-83)," American Concrete Institute, Farmington Hills, Mich., 241 pp.